4268–4275 *Nucleic Acids Research, 1994, Vol. 22, No. 20* © *1994 Oxford University Press*

Patterns of intracellular compartmentalization, trafficking and acidification of 5′-fluorescein labeled phosphodiester and phosphorothioate oligodeoxynucleotides in HL60 cells

John L.Tonkinson and C.A.Stein*
Department of Medicine, Columbia University, College of Physicians and Surgeons, 630 W. 168 Street, New York, NY 10032, USA

Received June 1, 1994; Revised and Accepted August 8, 1994

ABSTRACT

We have examined the intracellular compartmentalization and trafficking of fluorescein labeled (F) phosphodiester (PO) and phosphorothioate (PS) oligodeoxynucleotides (oligos) in HL60 cells. A series of F-oligos (PO and PS) were incubated for 6 hrs. with HL60 cells and the mean intracellular fluorescence determined by flow cytometry. The F signal was normalized by the addition of the ionophore monensin. An increase in signal intensity following addition of monensin indicated that the oligo was resident in an acidic intracellular environment. F-PS, but not F-PO oligos were found to reside in an acidic environment. An exception was a PO homopolymer of 15 cytidine bases (FOdC15) which was acidified. Using two different methods, the average resident intracellular pH of F-PS oligos and F-OdC15 was shown to be approximately 1 pH unit lower than that of F-PO oligos. Acidification of F-PS oligos could be blocked by the antibiotic bafilomycin, indicating that acidification was occuring in endosomes or vacuoles. F-PO and F-PS oligos were effluxed from HL60 cells from two intracellular compartments. However, approximately 60% of internalized F-PO oligo resided in a 'shallow' compartment that was turned over rapidly ($t_{1/2}$ = 5–10 min.) whereas only 20% of F-PS oligo resided in this compartment. Conversely, approximately 80% of the internalized F-PS oligo but only 40% of F-PO oligo resided in a 'deep' compartment that turned over with $t_{1/2}$ = 2–5 hrs. This report is the first quantitative demonstration that PO and PS oligos, and PO oligos of different sequences are trafficked differently by HL60 cells.

INTRODUCTION

Oligodeoxyribonucleotides (oligos), by virtue of the specificity of the Watson–Crick base pair interaction, have been proposed as antisense inhibitors of genetic expression, both *in vitro* and *in vivo* (for a recent review see ref. 1). While there are many examples in the literature that attest to the ability of the antisense oligo technology to specifically inhibit genetic expression, these successes, in our opinion, may represent only a small fraction of the experiments performed. Moreover, to cite one specific example, in spite of the fact that earlier data indicate that the expression of the c-*myc* oncogene can be selectively downregulated in HL60 cells (2–4), we and many others have had difficulty in reproducing these results. This lack of reproducibility may result from differences among investigators in several putatively controlled parameters. These may include 1) intrinsic differences between the HL60 cells, which are not clonal populations; it is also possible differences in the cell passage number may be significant; 2) differences in the composition of the fetal calf serum; and 3) differences related to the purity of the oligos; other factors, as yet unknown, also probably exist. Most critical, however, is the fact that the concentration of oligo in a relevant (with respect to antisense inhibition) intracellular compartment is as yet unknown. Furthermore, it is not possible to determine this concentration with any certainty unless patterns of intracellular oligo compartmentalization and trafficking are determined. In this work, we have examined the interaction of both 5′-fluorescein labeled (F) phosphodiester (PO) and phosphorothioate (PS) oligos with HL60 cells, and have examined parameters of cellular trafficking. These parameters include oligo acidification, and rates of their exocytosis from the cell. Consistent differences in intracellular trafficking, compartmentalization and efflux rates were observed between the 5′-F labeled PO and PS classes of oligos, and between F-PO oligos that differed in sequence. Entry into an acidic environment was also observed to be dependent on oligo class, and, to a lesser extent, on sequence. Finally, an average intracellular pH was determined for the different F-oligos. Using the data derived from these measurements, we constructed a mathematical model for the intracellular trafficking of 5′-F oligos in HL60 cells.

MATERIALS AND METHODS

Cells

HL60 cells were grown in a 5% CO_2 humid environment, in RPMI media/10% fetal bovine serum (Gibco, Grand Island, NY), supplemented with 0.1 mM MEM nonessential amino acids, 1

*To whom all correspondence should be addressed

mM pyruvate, 100 mg/mL penicillin, and 100 μg/mL streptomycin. The serum was heat inactivated at 65°C for 1hr. No degradation of PO oligos in serum so treated was observed after analysis by 7M urea polyacrylamide gel electrophoresis.

Reagents and chemicals

Monensin and nigericin were purchased from Sigma (St. Louis, MO) and were dissolved in 100% dehydrated ethyl alcohol. Bafilomycin was the generous gift of Dr M.Wax (Washington University, St. Louis, MO) and was dissolved in DMSO (Fisher, Pittsburgh, PA). Dilutions of monensin, nigericin and bafilomycin were made in sterile PBS. Fluorescein isothiocyanate (FITC), rhodamine isothiocyanate (RITC), and bo-dipy (4,4-difluoro-5-(4-phenyl-1,3-butadienyl)-4-bora-3a,4a-diaza-indacenepropionic acid, succinimidyl ester) 581/591 were purchased from Molecular Probes (Eugene, OR).

Synthesis of oligodeoxynucleotides

Phosphodiester oligonucleotides were synthesized by standard phosphoramidite chemistry on an Applied Biosystems (Foster City, CA) 380B synthesizer. Phosphorothioate oligos were also synthesized by standard methods, and sulfurization was performed using tetraethylthiuram disulfide/acetonitrile (TETD; Applied Biosystems). Following cleavage from the controlled glass support, oligos were base deblocked in ammonia hydroxide at 60°C for 8 hr. and purified by reversed phase HPLC (0.1M triethylammonium bicarbonate (TEAB)/acetonitrile, PRP-1 support). Oligomers were detritylated in 3% acetic acid and precipitated with 2% lithium perchlorate/acetone dissolved in sterile water, and reprecipitated as the sodium salt from 1 M NaCl/ethanol (5). Oligo concentrations were determined by spectroscopy.

5′-Modified oligos

5′-fluorescein (F) and 5′-rhodamine (R) labeled oligos. These oligos were synthesized as previously described (5). Oligomers to be fluorescently labeled were synthesized with either Aminolink 2 (Applied Biosystems) or with LCA (ABN, Hayward, CA) at the 5′ terminus according to the manufacturer's instructions. We observed no difference in properties between F-oligos synthesized with aminolink and F-oligos synthesized with LCA. The oligos were precipitated with 2% lithium perchlorate/acetone, reprecipitated as the sodium salt, dissolved in sterile water, and the concentration determined by UV spectroscopy.

5′-bo-dipy labeled oligos. Approximately 10 OD 260 units of 5′-aminolinked oligo dissolved in 100 μl of 100mM MOPS buffer, pH 7.4, were treated with 2 mg of bo-dipy N-hydroxysuccinimide ester dissolved in 10 μl DMSO. After 24 hours, the mixture was passed through a mini-column of Sephadex G-25, and the labeled oligo collected with the void volume. Further purification was achieved by electrophoresis on a 7M urea/20% polyacrylamide gel. The oligo band was excised and soaked for 24 hrs. in 0.1 M TEAB, and the eluate desalted over Sephadex G-25. The oligo was then precipitated with 2% $LiClO_4$/acetone, dissolved in sterile water, and the concentration determined by UV spectroscopy.

5′-F-1,6-hexanediammino-^{32}P-OdT15 (F-^{32}P-OdT15). This compound was synthesized by a modification of the method of Knorre and Vlassov (6). Briefly, after 5-phosphorylation of OdT15 by the Chemical Phosphorylation Reagent (Glen Research, Herndon, VA), a reaction exchanging the ^{32}P of [γ-^{32}P]ATP was carried out using T4 polynucleotide kinase with ADP as the phosphate acceptor (7) (sp. act. = 0.45 Ci/mmol). Then, 1,6-diamminohexane was coupled to the 5′ terminal ^{32}P by reaction with triphenylphosphine/dipyridyl disulfide. The product was then dissolved in 90 ml of 100 mM Na_2CO_3, pH 9.0. 1 mg FITC, dissolved in 10 ml of DMSO was then added. After 16 hrs., the mixure was extensively dialyzed against 0.1 M TEAB/1 mM EDTA. The product was further purified as described above. The molar ratio of F/oligo was approximately equal to unity as determined by UV/VIS spectroscopy.

Determination of efflux products of F-^{32}POdT15

HL60 cells (2×10^7) in 5 ml of complete media were treated with 5 μM of F-^{32}POdT15 for 3 hrs. 0.1 μM SdC28 was then added to remove cell surface bound F-oligo. The cells were then washed three times with cold PBS until the number of cpm in the media was background. The cells were then resuspended in Hank's balanced salt solution (HBSS) + 25 mM HEPES pH 7.1 (37°C), and aliquots of the media were then removed at the stated time points. The dissolved oligos were then precipitated by the addition of 10 volumes of a 2% solution of $LiClO_4$/acetone. >95% of the total ^{32}P-containing material was precipitated. The pellet, after centrifugation, was washed with acetone, dried, and dissoved in water and a three-volume excess of 1×TBE (pH 8.0)/90% formamide, and electophoresed on a 7 M urea/20% PAGE gel. The gel was allowed to expose Kodak X-200 film for 7 days at −80°C.

Flow cytometry

Following incubation for the stated times with the appropriate concentration of fluorescent oligo, cells were washed twice with PBS/BSA and resuspended in 300 μl PBS/BSA containing 0.3 μg/ml propidium iodide (PI). Relative fluorescence intensities were determined on a Becton−Dickinson FACStar Plus dual-laser flow cytometer using DESK software, as previously described (5). Following analysis, monensin (20 μM final) was added to each tube (15−30′), and the mean fluorescence intensity for a population of 5,000 cells was determined.

Efflux experiments

HL60 cells were plated at a density of 5×10^5/ml in 96-well microtiter plates, and incubated for at least 16 hrs. F-oligos were added to the cells at a final concentration of 5 μM. Following load time of the stated duration, the media was removed by centrifugation, and 200 μl cold PBS/BSA containing 0.1 μM SdC28 was added to each well. We have previously shown that the SdC28, because it competes for polyanion binding sites on the cell surface, effectively removes all surface bound F-oligo (5). Cells were allowed to sit for 1−2 min on ice at 4°C, centrifuged, and the supernatant removed. The cells were resuspended in 200 μl prewarmed media, and placed in the incubator for the stated efflux times (5′-3hr). Following efflux, the cells were washed two times in cold PBS/BSA, resuspended in 200 μl PBS/BSA and added to 100 μl PBS/BSA with 0.3 μg/ml propidium iodide. Mean fluorescence was determined by FACS as described above in the absence and presence of monensin.

Curve fitting

The efflux data obtained in the manner described above was fit to an exponential function by DeltaGraph Professional. Each curve was assumed to represent either a mono or biexponential function of the form $C_T = Ae^{(-\alpha t)}$ or $C_T = Ae^{(-\alpha t)} + Be^{(-\beta t)}$, where A and B represent the proportion of oligo in each compartment t = 0, and α and β are the rate constants for the loss of oligo from each compartment. The parameters were determined by multiple iterations so as to minimize the residuals, the only restriction being A, B, α, $\beta > 0$.

Intracellular pH measurements

The average intracellular pH of oligos was determined by a ratiometric measurement as described (8). 2×10^6 HL60 cells were incubated with F-oligo for 6 hrs. The cells were washed, and cold PBS containing 0.1 μM SdC28 was added for 2 min to remove all labeled oligo from the cell surface. In experiments using the SLM spectrophotometer, the cells were then resuspended in prewarmed media, placed at 37°C for 45′, and then washed twice with PBS. Subpopulations of 5×10^4 cells were placed in 3 ml of 132 mM K^+/20 μM nigericin-containing buffers of various pH, (10 mM MES, pH 5.5, 6 and 6.5; 10 mM HEPES, pH 7 and 7.5) or in PBS or Hanks balanced salt solution with HEPES buffer, pH 7.1, without nigericin. Fluorescent emission intensity from each population was determined on an SLM 48000 fluorescence spectrophotometer, using the excitation spectrum setting. Emitted light >515 nmeters was collected using a cutoff filter. Variations in lamp intensity were corrected for with a rhodamine standard. The light intensity at excitation wavelengths of 450 and 490 nm were detemined, and the 490/450 ratio plotted as a function of pH.

Intracellular pH could also be determined by a flow cytometric technique similar to the spectrophotometric method. The standard pH vs. F/B emission ratio measured at 488_{ex} for F and 581_{ex} for B was determined as a function of pH as described above. (The latter emission can be obtained from excitation with the argon laser). HL60 cells (10^5 cells/200 μl) were incubated with 2.5 μM BOdT15 (or BSdT15) + 2.5 μM FOdT15 (or 2.5 μM FSdT15) for 6 hr. The cell surface-bound oligo was removed with 0.1 μM SdC28 in PBS. The cells were washed, suspended in PBS, and fluorescence intensity determined in a least duplicate measurments. There was less than a 5% difference between the duplicates.

RESULTS

Acidification of 5′-F phosphodiester and phosphorothioate oligodeoxynucleotides

In our initial experiments, we used flow cytometry to attempt to determine if 5′-FOdT15 resided in an acidic environment. We took advantage of the fact that the 488_{ex} emission intensity of fluorescein is dramatically pH dependent. Thus, if the oligo was resident in a compartment of low pH, the addition of monensin (mon), which disrupts the pH gradient between the endosome and the cytoplasm, should cause a measurable increase in signal (9,10). As a control, we examined F-bovine albumin, which, like F-OdT15, is a marker of pinocytosis in HL60 cells. A sharp increase in signal was noted in HL60 cells that were incubated with 0.1 mg/mL F-bovine albumin + 20 μM mon. The signal also continued to increase as a function of time. On the other hand, even up to 18 hrs., no increase in signal was seen when cells were treated with 5–15 μM 5′-FOdT15. The behavior of F-bovine albumin vs. 5′-F-OdT15 was different even when corrected for mol fluorescein bound/mol protein. These data suggested that, unlike F-bovine albumin and F-transferrin, which we also found to be acidified, as has been previously described (11), F-OdT15 did not at any time (up to 18 hrs.) appear to reside in an acidic environment.

We then determined if other F-oligos behaved similarly. We

Table 1. Fluorescently labeled oligonucleotides

F-OdT_{15}	F-OdC_{15}	F-SdT_5
F-Od$C_{10}T_5$	F-OdT_{20}	F-SdT_{15}
F-Od$(CT)_7$C	F-OdC_{20}	F-SdC_{15}
F-OdA_{15}	F-Od$C_{15}T_5$	F-SdT_{28}
FOd$(AC)_7$C	F-OdT_{12}SdT_3	

F=Fluorescein; O=Phosphodiester; S=Phosphorothioate; d=Deoxy; T=Thymidine; C=Cytidine; A=Adenine.

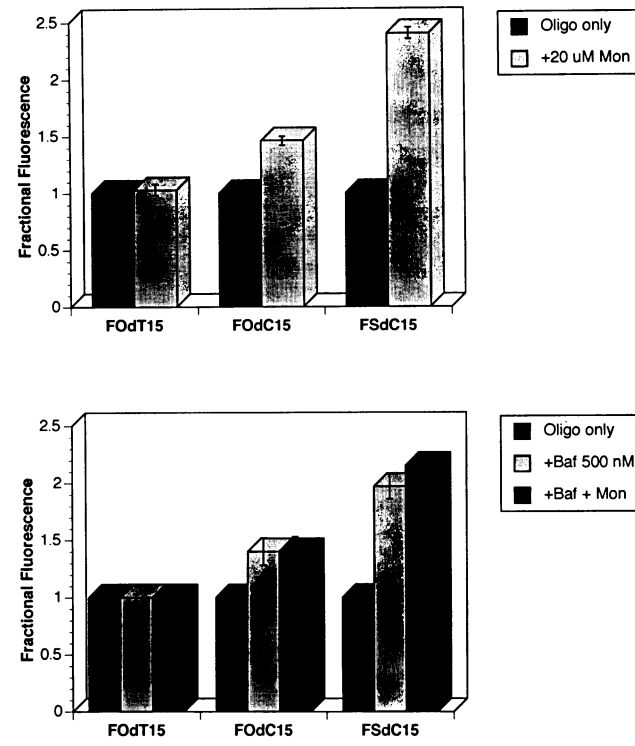

Figure 1. Selective intracellular acidification of oligonucleotides. Top panel: HL60 cells were incubated at 37°C for 6 h. (RPMI 1640/10% FBS) with 5 μM F-oligo. The cells were washed and the mean linear fluorescence intensities for each treatment were determined by FACS analysis (black bars). Then, monensin (20 μM final) was added to each sample, and the mean linear fluorescence intensities redetermined (gray bars). Bottom panel: Where indicated, the macrolide antibiotic bafilomycin (baf) (500 nM) was included in the incubation. Following FACS analysis, monensin was added to each sample, and the mean fluorescence redetermined. The signal intensities are plotted as fractions relative to the control sample (− mon) for each treatment. Error bars represent the standard deviations for triplicate measurements.

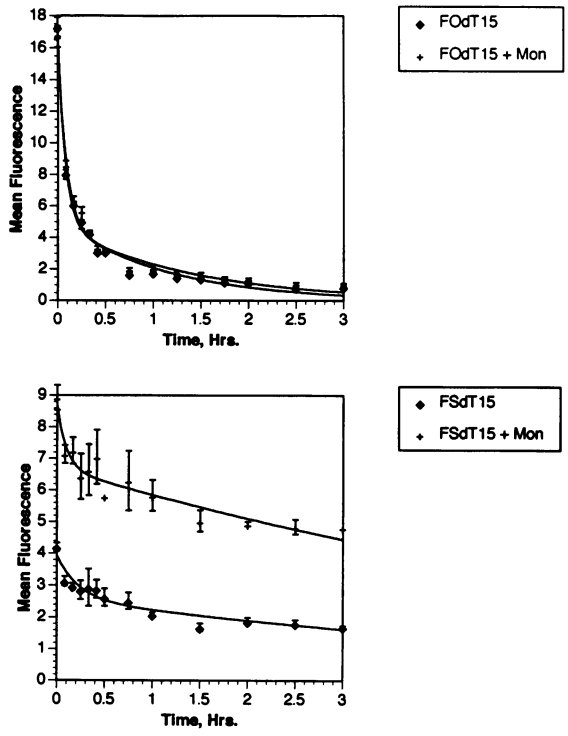

Figure 2. PO and PS oligos are effluxed from HL60 cells at different rates. HL60 cells were incubated at 37°C for 6 h. (RPMI 1640/10% FBS) with 5 μM F-OdT15 (top panel) or 5 μM F-SdT15 (bottom panel). After washing, the surface bound oligo was removed (see 'Materials and Methods'). The cells were resuspended in warm media, placed at 37°C for the indicated times, washed and then analyzed by flow cytometry. After analysis, monensin (20 μM final) was added to each sample, and the mean linear fluorescence for each time point was redetermined. The signal intensities (arbitrary fluorescence units) are plotted as a function of time, and the data were fit to the biexponential function $C_T = Ae^{-\alpha t} + Be^{-\beta t}$ by Delta Graph as described in the text. Error bars represent the standard deviation of triplicate measurements.

examined a series of F-oligos, which are given in Table 1. These data are presented in Figure 1. No F-PO oligo that we examined was found to reside in an acidic environment; the single exception to this was 5′-F-OdC15. In striking contrast, the three PS oligos examined all resided in acidic compartments, and addition of monensin produced a sharp increase in intracellular fluoresence.

In order to demonstrate that the monensin-induced increase in fluorescent signal was caused by acidification of an endosomal compartment, we used the macrolide antibiotic bafilomycin to inhibit the activity of the vacuolar ATPase. This ubiquitous protein is found in the endosomal membrane of virtually all mammalian cells, and, in a ATP-dependent manner, pumps protons into the endosomal lumen (12). Bafilomycin (baf) is thought to be a specific inhibitor of this protein, and has been shown to block endosomal acidification in mammalian cells (13). We treated HL60 cells with 500 nM baf and 5 μM F-oligos as shown in Figure 1. F-OdT15, which never appears to be acidified, does not give an increased signal relative to control with the inclusion of baf in the incubation period. On the other hand, a striking increase in signal is observed when baf is included in the incubation period with F-SdC15 and F-SdT15 (not shown). Furthermore, treatment with 20 μM mon did not further increase the signal, suggesting that the internal endsomal pH was similar

Table 2. Parameters for the bi-exponential loss of F-oligo from HL60 cells

	A	α	B	β
F-PO (15-20mer)	61.0 +/- 4.0	10.0 +/- 2.7	36.4 +/- 4.3	0.329 +/- 0.053
F-PO/PS (15mer)	67.0 +/- 2.5	9.4 +/- 3.8	32.4 +/- 2.5	0.504 +/- 0.114
F-PS (15-28mer)	18.6 +/- 3.7	3.5 +/- 1.0	80.4 +/- 4.4	0.131 +/- 0.061
F-OdC15	28.6 +/- 1.4	15.6 +/- 5.7	71.3 +/- 1.6	0.168 +/- 0.028
F-PS + Baf	29.4 +/- 5.7	14.4 +/- 12.9	66.8 +/- 9.6	0.100 +/- 0.051
F-OdC15 + Baf	35.5 +/- 2.2	19.9 +/- 3.7	63.7 +/- 2.6	0.173 +/- 0.115

The parameters for the bi-exponential loss of F-oligo from HL60 cells were determined as described in the text, ($C_T = Ae^{-\alpha t} + Be^{-\beta t}$). The coefficients 'A' and 'B' represent the percentage of F-oligo in each compartment following a 6 h incubation; 'α' and 'β' are the rate constants (h^{-1}) for the loss of F-oligo from each compartment. Average values were determined for the oligos listed in Table 1. F-PO/PS is a chimeric oligo (FOdT12SdT3) with three PS linkages at the 3′ end. Baf = bafilomycin (500 nM) which was included in the uptake period and the efflux period.

to that of the cytoplasm. F-OdC15, which appeared to be acidifed in our preliminary experiments, did produce an increased signal in the presence of baf, also suggesting that endosomal acidification had occurred.

Exocytosis of 5′-F oligos from HL60 cells

In order to better understand differences in intracellular trafficking between different classes and sequences of oligos, we studied the rate at which they underwent exocytosis from HL60 cells. We have prevously found that the steady-state accumulation of F-oligo is reached in HL60 cells by 3–6 hours. Thus, we performed most of our experiments at a load time of 6 hours. However, the measured rate of exocytosis of F-oligo from HL60 cells appeared to be invariant with respect to a load time of from 3–6 hours. A representative plot of the rate of loss of fluoresence from HL60 cells as a function of time is shown in Fig. 2. In Fig. 2 (top), the loss of F-OdT15 best fits a bi-exponential function of the form $C_T = Ae^{-\alpha t} + Be^{-\beta t}$. (It is possible that a third exponential term, $Ce^{-\gamma t}$, can also be included, but it is not required for a best fit). The individual exponential terms may be referred to as compartments or phases, but they do not necessarily correspond to biological structures. The coefficients A and B represent the size of the individual compartments, and the terms α and β represent the kinetic constants for the loss of material from the cells. For F-OdT15, approximately 61% of the material was found in the A, or 'shallow' compartment (relatively rapid efflux, short $t_{1/2}$), and about 36% was found in the B, or 'deep' compartment. (relatively slow efflux, long $t_{1/2}$; Table 2).

For F-OdT15, on addition of 20 μM mon, the fluorescent intracellular signal did not change in intensity at any measured time points. In sharp contrast (Fig. 2 bottom), when we examined the exocytosis of F-SdT15, a dramatic increase in signal intensity was observed at all time points studied. Because this effect is due to acidification of the PS oligo in a vacuolar compartment, the true efflux rate is given in Fig. 2 (bottom) by the upper curve. These data can best be described by either a bi- or a mono-exponential function. The values of the kinetic constants for the bi-exponential function are given in Table 2. For F-SdT15, about

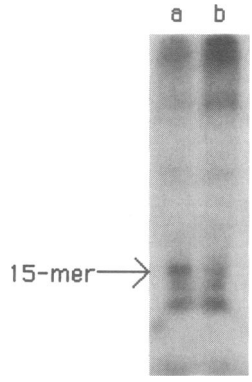

Figure 3. Efflux products of F-^{32}P-OdT15. HL60 cells were incubated at 37°C for 3 h. with 5 mM F-^{32}P-OdT15 (RPMI 1640/10% FBS). Surface bound oligo was removed and the cells were washed until the number of cpm in the media was background. The cells were resuspended in warm HBSS/HEPES and placed at 37°C. Aliquots of the media were removed at 2 h. (a) and 3 h. (b). The dissolved oligos were precipitated with $LiClO_4$, and analyzed on a 7 M urea/20% PAGE gel. The arrow indicates the mobility of full length oligo.

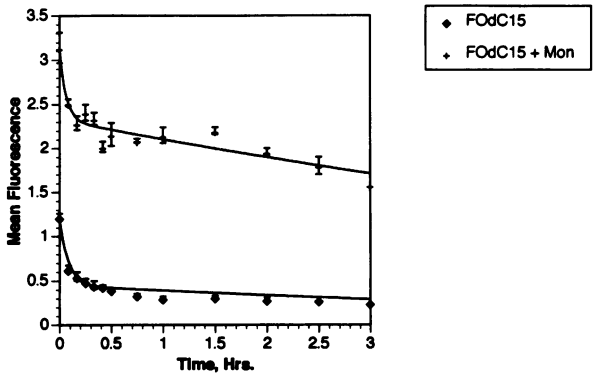

Figure 4. The rate of exocytosis of F-OdC15 is similar to that of F-PS oligos. HL60 cells were incubated at 37°C for 6 h. (RPMI 1640/10% FBS) with 5 μM F-OdC15. After washing, the surface bound oligo was removed, and the cells were resuspended in warm media and placed at 37°C. At the indicated times, the cells were washed and the mean linear fluorescence intensity for each time point was determined by FACS. Following analysis, monensin (20 μM) was added to each sample, and the mean fluorescence for each population redetermined. The mean fluorescence intensities are plotted as a function of time, and the data were fit to a biexponential function by Delta Graph as described in the text. Error bars represent the standard deviation of triplicate measurements.

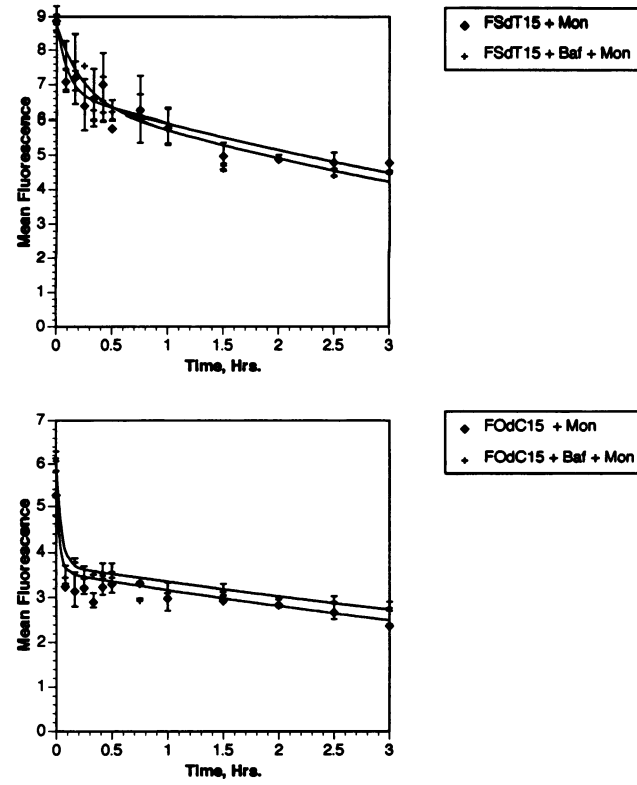

Figure 5. The rate of F-oligo efflux is independent of acidification. The efflux kinetics of F-SdT15 (top panel) and F-OdC15 (bottom panel) were determined in the absence and presence of bafilomycin (baf) (500 nM). HL60 cells were incubated at 37°C for 6 hrs. (RPMI 1640/10% FBS) with 5 μM F-oligo; parallel samples also contained baf. After washing, cell surface bound oligo was removed and the cells were resuspended in warm media with or without baf., and placed at 37°C. At the indicated times, the cells were washed and the mean linear fluorescence for each population was determined by FACS. Monensin (20 μM final) was then added to each sample, and the fluorescence redetermined. The mean fluorescence values are plotted as a function of time, and the data were fit to a biexponential function as described previously. The error bars are the standard deviations from triplicate measurements.

19% of the material was found in the A or 'shallow' compartment. About 80% was found in the B, or 'deep' compartment. Thus, the relative sizes of the shallow and deep compartments for the PS and PO oligos are virtually reversed. However, despite differences in the observed rate of loss, the intrinsic rate of loss of material from a specified compartment was almost identical, regardless of oligo class (F-PO vs. F-PS) and length. Furthermore, we also examined the efflux kinetics of R-OdT15 and R-SdT15. For R-OdT15, the rate of loss of rhodamine fluorescence from the HL60 cells was identical to that for F-OdT15 (data not shown). For R-SdT15, the rate of loss of rhodamine fluorescence from the HL60 cells was identical to that of F-SdT15 after treatment with mon (data not shown). These data suggest that our observed effects were only minimally dependent on the nature of these 5′-fluorescent groups. We also examined the efflux of free fluorescein sodium from HL60 cells, and the rate was much greater than for any F-oligo examined in this study.

In order to demonstrate that the loss of fluorescence was correlated with the loss of oligo, we determined the efflux products of 5′F-^{32}P-OdT15. This compound is stable in heat-inactivated media, and does not undergo any digestion with bacterial alkaline phosphatase up to 12 hours (data not shown). The efflux products are shown in Fig. 3. The load time was 3 h, and the measurement times were two and three hours. Significant amounts of full length 15-mer were observed. Shortened and chain-extended oligos were also seen, as well as high-molecular weight material which may not represent oligo. Due to the much greater stability of the PS oligos at these efflux time points, as previously reported, their efflux products were not examined.

All of the PO oligos that we have examined, irrespective of

Table 3. Average intracellular pH of F-oligos in HL60 cells: a comparison of methods

Oligo	Method Spectrophotometric (490/450)	FACS (F/B)
FOdT15	7.1 +/− 0.3 (n = 5)	7.2 +/− 0.1 (n = 5)
FOdC15	6.3 +/− 0.2 (n = 3)	6.4 +/− 0.04 (n = 3)
FSdT15	6.1 +/− 0.2 (n = 3)	6.3 +/− 0.09 (n = 5)
FSdC15	6.4 +/− 0.1 (n = 3)	------

Spectrophotometric method: 2×10^6 HL60 cells were incubated with F-oligo (5 μM) for 6hr. After cell surface F-oligo was removed as described in 'Materials and Methods' the cells were placed in warm media for 45 min., and then washed extensively in cold PBS. Subpopulations of 5×10^4 cells were placed in 3 ml of high K^+, nigericin containing buffers of various pH, or in Hanks buffered HEPES pH 7.1 without nigericin. Emission intensities at excitation wavelengths of 490 nm and 450 nm were determined on a fluorescent spectrophotometer as described above. The average pH was determined by comparing the 490/450 ratio from the Hanks/HEPES sample to the standard curve of 490/450 vs. pH. A unique standard curve was generated for each oligo.

Flow cytometric method: populations of HL60 cells (1×10^5/200μl) were incubated for 6 h with 2.5μM F-oligo + 2.5μM B-oligo. Following incubation, surface bound oligo was removed and the cells were washed extensively. The cells were placed in high K^+ nigericin containing buffers of various pH, or in PBS, pH 6.8. Mean fluorescent intensities for each population were detemined on a FACStar Plus flow cytometer as previously described. The average pH was determined by comparing the F/B ratio from the PBS sample to the standard curve of F/B vs. pH. A unique standard curve was generated for each oligo.

length or sequence, (Table 1), show efflux behavior similar to F-OdT15. However, the efflux behavior of F-OdC15 was in striking contrast to this. F-OdC15 resided in an intracellular acidic environment, as shown in Figure 1. Treatment with 20 μM mon produced a sharp increase in fluorescent signal; thus, the true rate of efflux, as for PS oligos, could only be determined in the presence of monensin (Fig. 4 top curve).

In order to examine the relationship between acidification and efflux, we determined the rate of loss of FSdT15 and FOdC15 in the presence of bafilomycin (baf) (Fig. 5; Table 2). Treatment with baf changed neither the coefficients A and B, nor the rate constants α and β. These data suggest that acidification is not, *a priori*, responsible for the slow efflux of these oligos. Rather, these data suggest that it is the slow efflux that may lead to ultimate F-oligo acidification.

The rate of efflux and acidification of PS oligos appears to change as oligo length diminishes. Following a 6 h. incubation of F-SdT5 with HL60 cells, mon treatment resulted in only a slight increase in fluorescence. This indicates that F-SdT5 is not acidified to the same extent as longer F-PS oligos. We then examined the kinetics of efflux of F-SdT5. The coefficients A and B were almost identical, indicating that equal amounts of F-SdT5 resided in both the shallow and deep compartments. The observed efflux rate is slower than the F-PO but faster than the F-PS oligos.

Determination of intracellular pH

The determination of intracellular pH was performed by two methods:

Spectrophotometric method. A unique calibration curve was constructed for each F-oligo and the 490/450 ratio determined as described above. The data points (not shown) were fit to a straight line using Delta graph (r^2 = 0.984). The average intracellular pH of F-SdT15 was 6.1 +/− 0.2 (n = 3). The values of average pH for other F-oligos is given in Table 3. It should be noted that these data represent a weighted biased pH average; this is so because it is not likely that all of the intracellular F-oligo resides at the measured pH. It is likely that some F-oligo resides at both higher and lower values of pH.

Flow cytometric method. This was performed using the emission ratio of F_{488ex}/B_{581ex}. Due to problems of fluorescence energy transfer between the fluorochoromes, we found that it was not possible to employ R as the 5′-fluorescent label for these measurements. This problem was solved using the 5′-linked bodipy fluorochrome; this is a polyalkene fused bis-pyrazolo fluoborate which does not undergo significant energy transfer with F, and whose emission is, like R, relatvely pH independent. Standard curves were constructed for each oligo as described above. The average intracellular pH of F-OdT15 was determined to be 7.2 +/− 0.1 (n = 5); for F-SdT15, the pH was 6.3 +/− 0.09 (n = 5). These values are similar to those determined by Method 1 (Table 3), and are consistent with our previous data that suggest that F-PS, as opposed to F-PO oligos, reside in an acidic intracellular compartment.

DISCUSSION

The use of fluorescein as a marker has allowed us and others (5,14,15) to use flow cytometry to measure the cellular uptake of oligos. By using this technique, each cell can be analyzed individually, and dead cells, which appear to accumulate polyanions, can be gated out of the final data analysis. However, the use of fluorescein as a marker may produce artifactual results. One reason for this is because the extinction coefficient of fluorescein varies with pH. Thus, observed variations in signal intensity may not be a true reflection of differences in intracellular concentration of oligo, but instead may reflect differences in oligo compartmentalization.

We have demonstrated that PS oligos appear to enter an acidic intracellular environment, but PO oligos do not. Furthermore, PS oligos are retained within the HL60 cell for relatively long periods of time (> 70% turns over with $t_{1/2}$ = 3 hrs) (16), but PO oligos appear to be effluxed rapidly (> 60% turns over with $t_{1/2}$ = 5 min).

Although the mathematical compartments identified in this work have not yet been absolutely defined physiologically, confocal microscopic data we have obtained indicates that both F-PO and F-PS oligos reside in vesicular structures. The observed acidification of F-PS oligos indicates that they are sequestered in endosomes or lysosomes; in such a location, they are thus not available for interacting with mRNA. It appears possible that such sequestration in HL60 cells represents a physiological 'dead end' for F-PS oligos. The F-oligos (both PO and PS) which do not reside in an acidic compartment could either be located in the cytoplasm or nucleus or both; alternatively they could undergo efflux from the cell prior to acidification of the pinosomes. Our data suggests that the latter represents a significant mode of F-oligo trafficking in HL60 cells, especially in the case of F-PO oligos.

Previous work has focused on the mechanism by which oligos are internalized by cells (5,17). These studies, which have employed radioactive as well as fluorescently labeled oligos, are

in general agreement that the internalization process involves a combination of adsorbtive endocytosis plus pinocytosis. Firm evidence for internalization by the process of potocytosis, as has previously been suggested, is at the present time lacking (18). The internalization process of pinocytosis, in which bulk extracellular fluid is constitutively engulfed by the cell, occurs at variable rates between cell types, and appears to be dependent on the metabolic state of the cell. Studies using markers of the fluid phase such as fluorescent dextran or horseradish peroxidase (HRP) have demonstrated that pinocytosed molecules enter an endocytic pathway and are either recycled to the medium or proceed toward lysosomal sequestration (19,20). Detailed studies of the exocytosis of pinocytosed molecules have revealed that at least two mathematical compartments may be defined (21,22). Exocytosis of the markers is observed from each compartment. The first compartment turns over with $t_{1/2} = 5-10$ min. and the second compartment with $t_{1/2} = 180-480$ min. Although the observed rate constants for the efflux from each compartment are similar in all reported studies, the relative amount of material residing in each compartment is dependent on cell type and marker. For example, Besterman *et al.* (21) found that in alveolar macrophages and in fetal lung fibroblasts, the relative amount of ^{14}C-sucrose in each compartment varied with load time. The 'size' of the first compartment decreased with increasing load time, such that after a 180′ load, 90% of the sucrose was in the compartment with slower turnover: This resulted in an observed slow efflux rate. By contrast, Blomhoff *et al.*,(22) reported that 80% of pinocytosed ^{125}I-poly(vinylpyrrolidone) (PVP) resided in the first compartment of liver parenchymal cells, resulting in an observed rapid efflux rate.

We wish to stress that it would not be appropriate to extrapolate these data to other cell lines. There is also a possibility that the presence of the 5′-F label affects the net behavior of the F-oligo complex. However, it appears more likely that this perturbation, based on the ability of fluorescein to interact hydrophobically with lipid membranes, is relatively small. Evidence for this contention consists in our studies of the binding of 5′ F-PO and PS oligos to the cell surface of HL60 cells, presumably to p80 or variants (5). This binding is strongly competitive with unmodified PO or PS oligos. In contrast, when the 5′ modification is the cholesteryl moiety, which can interact directly with LDL and with cell membranes, the binding to the cell surface is only partially competed by unlabeled oligo, even in the absence of exogenous LDL (23). Furthermore, the values of K_d for the cell surface binding of F-labeled and unlabeled PO and PS oligos are similar. In addition, the efflux rates of the F and R-oligos, which bear different charges at their 5′ termini, are virtually identical. The behavior of 5′-F oligos, while perhaps not identical to that of unlabeled oligos, may nevertheless represent a useful approximation.

The study of the intracellular behavior of PO oligos is complicated by the fact of nuclease digestion. This is believed to occur predominately in a 3′−5′ direction by exonuclease activity (24). Our studies on the exocytosis of F-PO oligos indicated that a significant amount of the internalized material underwent such digestion. Thus, the kinetic model as depicted in Figure 2 represents only a limiting description of the behavior of F-PO oligos. However, we also examined the efflux characteristics of a chimeric oligo (Table I) that contained three PS groups at the 3′ terminus; these are sufficient to significantly block 3′−5′ exonuclease activity (25). The efflux kinetics of this oligo were virtually identical to those of the non-chimeric PO oligos. On the other hand, the greatly increased nuclease stability of PS oligos significantly obviates problems with nuclease digestion. This is reflected in the work of Fisher *et al.*,(26) who have reported on the intracellular availability and integrity of oligos microinjected into mammalian cells. Fluorescently labeled oligos were found to accumulate in the nucleus following injection. The signal from the injected PO oligos disappeared rapidly ($t_{1/2} = 15-20$ min) but the signal from the injected PS oligos persisted in the nucleus for more than 24 hrs. Temsamani, *et al.* (27) using human 293 cells, found that only about 15% of an intracellular 20-mer PS oligo had been digested after 16 h, and that after 8 h all of the efflux products were essentially the full-length species.

We have previously utilized SdC28 at low concentration to remove cell surface bound F-PO and F-PS oligo (5). The advantage of this method is that it is rapid, highly reproducible, does not involve pH changes, and is non-toxic. The disadvantage is that SdC28 remains bound to the surface. It is possible that this may, by an as yet unknown mechanism, affect rates of oligo internalization and patterns of intracellular trafficking. Alternatively, the additional treatment of cells with SdC28 that have already been exposed to an F-oligo may not have great significance, because, as we have previously shown, after 6 hrs few oligo binding sites remain on the surface of the HL60 cell. Furthermore, the kinetics of exocytosis of F-SdT28, where a 28-mer is continuously present, differs little from that of F-SdT15 and F-SdC15.

The kinetics of exocytosis of F-SdT5, as described previously, are different than those of longer F-PS oligos. We speculate that the reason for this may lie in the relative protein binding abilities of oligos of different chain lengths. We have previously shown that the ability of PS oligos to bind to rsCD4 (28), gp120 (29), and p80 (5) depends greatly on oligo length. It is also frequently, although by no means universally true, that the value of K_d for a PS oligo/protein complex is about two orders of magnitude lower than that of the corresponding PO oligo. Diminished association with intraendosomal proteins may, in theory, create internalization problems for other classes of oligos. For example, both peptide nucleic acids (PNA), and methylphosphonate (MP) oligos, both of which have little, if any protein binding capability, appear to be internalized poorly (30,31). Poor intracellular retention, among other factors (e.g., lack of ability to elicit RNAse H activity) may relate to the relatively low antisense potency of these uncharged species.

Finally, answers to the critical questions of 1) the rate of passage of the oligo from the endosome into the relevant cellular compartment (i.e., nucleus or cytoplasm), and 2) the true oligo concentration in those relevant compartments are not currently known. However, in order to achieve, in a general way, the goal of maximization of antisense efficacy, it is necessary to proceed with experiments that will generate reasonable answers to these problems.

ACKNOWLEDGEMENTS

C.A.S. is the Irving Assistant Professor of Medicine and Pharmacology, Columbia University. This work was partially funded by NCI R29 60639.

REFERENCES

1. Stein, C.A. and Cheng, Y.C. (1993) Science 261, 285–288.
2. Wickstrom, E.L., Bacon, T.A., Gonzalez A., Freeman, D.L., Lyman, G.H., Wickstrom, E. (1988) Proc. Natl. Acad. Sci., USA 85, 1028–1032.
3. Holt, J., Redner, R., and Nienhuis, A. (1988) Mol. Cell. Bio. 8, 963–973.
4. Loke, S.L., Stein, C., Zhang, X., Avigan, M., Cohen, J., and Neckers, L.M. (1988) Current Topics in Microbiology and Immunology 141, 282–289.
5. Stein, C.A., Tonkinson, J.L., Zhang, L.M., Yakubov, L., Gervasoni, J., Taub, R., and Rotenberg, S. (1993) Biochemistry 32, 4855–4861.
6. Knorre, D.G., Vlassov, V.V., Zarytova, V.F., and Karpova, G.G. (1985) Adv. Enzyme Regul. 24, 277–300.
7. Sambrook, J., Fritsch, E., and Maniatis, T. (1989) Molecular Cloning: A Laboratory manual, p. 10.66, Cold Spring Harbor Laboratory, Cold Spring Harbor, NY.
8. Ohkuma, S. and Poole, B. (1978) Proc. Natl. Acad. Sci., USA 75, 3327–3331.
9. Maxfield, F.R., (1982) J. Cell Biol. 95, 676–681.
10. Maxfield, F.R., (1985) Endocytosis, Pastan, I., and Willingham, M.C., eds. Plenum Press, NY, 235–257.
11. Yamashiro, D.J. and Maxfield, F.R. (1984) J. Cell. Biochemistry 26, 231–246.
12. Nelson, N. (1991) Trends in Pharmacol. Sci. 12, 71–75.
13. Yoshimori, A., Yamamoto, A., Moriyama, Y., Futai, M. and Tashiro, Y. (1991) J. Biol. Chem. 266, 17707–17712.
14. Loke, S.L., Stein, CA., Zhang, X.H., Mori, K., Nakanishi, M., Subasinghe, C., Cohen, J.S. and Neckers, L.M. (1989) Proc. Natl. Acad. Sci. USA 86, 3474–3478.
15. Marti, G., Egan, W., Noguchi, P., Zon, G., Matsukura, M. and Broder, S. (1992) Antisense Res. and Dev. 2, 27–39.
16. Gao, W.Y., Storm, C., Egan, W. and Cheng, Y.C. (1993) Mol. Pharmacol. 43, 45–50.
17. Yakubov, L., Deeva., E., Zarytova, V., Ivanova, I., Ryte, A., Yurchenko, L. and Vlassov, V. (1989) Proc. Natl. Acad. Sci. USA 86, 6454–6458.
18. Zamecnick, P., Aghajanian, J., Zamecnick, M., Goodchild, J. and Witman, G. (1994) Proc. Natl. Acad. Sci. USA 91, 3156–3160.
19. van Deurs, B., Ropke, C. and Thorbal, N. (1984) European J. Cell Biol. 34, 96–102.
20. Adams, C.J., Maurey, K.M. and Storrie, B. (1982) J. Cell Biol. 93, 632–637.
21. Besterman, J.M., Airhart, J.A., Woodworth, R.C., and Low, R.B. (1981) J. Cell Biol. 91, 716–727.
22. Blomhoff, R., Nenseter, M.S., Green, M.H., and Berg, T. (1989) Biochem. J. 262, 605–610.
23. Krieg, A.M., Tonkinson, J., Matson, S., Zhao, Q., Saxon, M., Zhang, L.M., Bhanja, U., Yakubov, L. and Stein, C.A. (1993) Proc. Natl. Acad. Sci., USA 90, 1048–1052.
24. Dagle, J.M., Weeks, D.L. and Walder, J.A. (1991) Antisense Res. and Dev. 1, 11–20.
25. Stein, C.A., Subasinghe, C., Shinozuka, K., Cohen, J.S. (1988) Nucleic Acids Res. 16, 3209–3221.
26. Fisher, T.L., Terhorst, T., Cao, X. and Wagner, R.W. (1993) Nucleic Acids Res. 21, 3857–3865.
27. Temsamani, J., Kubert, M., Tang, J., Padmapriya, A. and Agrawal, S. (1994) Antisense Res. and Dev. 4, 35–42.
28. Yakubov, L., Khaled, Z., Zhang, L.M., Truneh, A., Vlassov, V. and Stein, C.A. (1993) J. Biol. Chem. 268, 18818–18823.
29. Stein, C.A., Cleary, A.M., Yakubov, L. and Lederman, S. (1993) Antisense Res. and Dev. 3, 19–31.
30. Nielsen, P., Egholm, M., Berg, R. and Buchardt, O. (1991) Science 254, 1497–1500.
31. Shoji, Y., Akhtar, S., Perisamy, A., Herman, B. and Juliano, R.L. (1991) Nucleic Acids Res. 19, 5543–5550.